

Copper Smelting Slag Cleaning in an Electric Furnace by Using Waste Cooking Oil



YONGGANG WEI, TIFU ZHANG, BO LI, and SHIWEI ZHOU

In view of the non-renewable reductant resources and carbon neutralization in the process of copper slag cleaning in an electric furnace, this study proposed to use waste cooking oil as reductant to replace fossil energy. Combined with the phase equilibrium theory and experimental results, the harm of excessive magnetite in the copper smelting slag to the cleaning process was clarified. The reduction thermodynamics of magnetite by using WCO is analyzed. A series of copper slag cleaning experiments with different WCO dosages along with various temperatures and settling durations was systematically carried out in a laboratory-scale electric furnace. The distribution of matte particles in each slag layer after cleaning was investigated in detail, which indicates that the copper content in the upper slag layer can be reduced to 0.56 wt pct *via* WCO reduction, realizing the green cleaning of copper slag.

<https://doi.org/10.1007/s11663-020-01986-7>

© The Minerals, Metals & Materials Society and ASM International 2020

I. INTRODUCTION

THE process of smelting combined with converting is becoming the main technology for blister copper production. Modern smelting technology injects oxygen-enriched air into the melt for efficient production of high-grade matte, and magnetite is inevitably precipitated in the melt as a result, leading to the increase in copper content of the slag.^[1] Therefore, copper slag cleaning is a critical process to reduce copper loss and improve copper recovery simultaneously. Copper slag cleaning using the flotation method and/or in an electric furnace is widely adopted in industrial production.^[2–5] The flotation method has the advantages of low energy consumption and low copper content in the slag,^[4] but the waste liquid treatment after flotation has always been an issue. Due to the simple process and high production efficiency, copper slag cleaning in an electric furnace is also favored in the copper industry.^[3] Local conditions (including the economic and environmental strategy), practical experience and smelting furnace characteristics should be considered for selecting the slag cleaning method.

The ISASMELT furnace is a typical representative smelting technology, which has the characteristics of continuous production and periodic discharge of matte. Because the matte and slag are tapped simultaneously from the same taphole, the slag cleaning furnace becomes the necessary equipment to promote separation of the matte from the slag. Too much magnetite content in the slag is the critical factor to hinder the matte particle settling,^[1] which makes it necessary to add an appropriate amount of reductant to the melt during the process of slag cleaning in the furnace. Based on the physicochemical reaction of the melt, the process of copper slag cleaning in an electric furnace could be divided into two steps: reduction and settling. In the reduction stage, excessive magnetite is reduced to provide favorable conditions for the settling. Natural gas, coal, coke, petro-diesel, ferrosilicon, *etc.*, were used as reductants to realize the objective conventionally,^[2] all with different degrees of success. In terms of resource characteristics, non-renewability seems to be their common defect, and they would emit additional environmentally unfriendly gases (CO₂, SO₂) during the reduction process. Furthermore, the ash in the coal and coke also enters the slag phase to increase the slag amount, and the total copper loss is increased as a result.

The use of biomass energy as an alternative source for reduction is promoted because of its sustainability and environmental protection. It has been reported that using biomass or biochar as reductant can effectively reduce the iron phase in ore or slag.^[6–8] Waste cooking oil is a by-product of human life. In China, millions of tons are produced every year because of the improvement of living standards.^[9] At present, the resource

YONGGANG WEI is with the State Key Laboratory of Complex Nonferrous Metal Resources Clean Utilization, Kunming University of Science and Technology, Kunming 650093, P.R. China. Contact e-mail: weiygcp@aliyun.com TIFU ZHANG is with the Yimen Copper Co., Ltd., Yuxi 651100, P.R. China. BO LI and SHIWEI ZHOU are with the Faculty of Metallurgical and Energy Engineering, Kunming University of Science and Technology, Kunming 650093, P.R. China.

Manuscript submitted May 20, 2020; accepted September 22, 2020.

Article published online October 16, 2020.

utilization of WCO is mainly to produce biodiesel, which is both technologically and economically feasible.^[10] High oxygen levels within WCO result in the low calorific value of biodiesel.^[11] In addition, research and development of downstream products in the chain of biodiesel production are lacking investment. Therefore, it is of great significance to develop a variety of effective technologies for the utilization of WCO to avoid environmental pollution.

Previous research^[12] indicated that 1 mL of WCO at 1300 °C would produce approximately 1180.3 mL of H₂ and 169.0 mL of CO by cracking. Approximately 80 pct of the carbon element within WCO was deposited as solid carbon. Therefore, 1 L of WCO can reduce at least 19.46 kg of Fe₃O₄ to FeO at 1300 °C (only H₂, CO and C produced by cracking were used as reductants), which can replace 2.4 kg of coke (fixed carbon content was approximately 85 wt pct) based on the theoretical calculation. From an environmental perspective, WCO is a renewable resource and can achieve zero carbon emissions during the entire lifecycle; coke is a non-renewable resource releases additional CO₂ and SO₂ during the reaction, putting pressure on the environment. From an economic viewpoint, the market prices of coke and WCO are approximately 1850 and 3500 CNY/ton, respectively; 1 L of WCO (approximately 0.914 kg) however can replace 2.4 kg of coke, so it is more economical to use WCO. Using waste oil as a reductant seems to be in line with the requirements of renewable sustainable development and environmental protection.

In view of the non-renewable reductant resources and carbon neutralization in the cleaning process, this study proposes to replace fossil reductants with liquid WCO. To promote this technology effectively, the reduction thermodynamics was first analyzed. Then, the influence of parameters changes in the reduction and settling process on the cleaning effect was systematically investigated, and the relationship between magnetite and copper content in the slag during the cleaning process using WCO was clarified. The results obtained in the present research may promote the application of WCO to the process of copper slag cleaning and provide a new approach to WCO utilization.

II. EXPERIMENTAL

A. Materials

1. ISASMELT copper slag

A representative ISASMELT copper slag sample was obtained from Copper Inc. in China. A mixture of matte and slag tapped from the ISASMELT furnace is a periodic operation. The mixture mainly consists of matte at the early stage during tapping, and then it changes into a mixture dominated by slag at the later stage. In the present investigations, the slag-matte mixture remaining on the chute after tapping was taken as the research object. Chemical analysis results of this sample are listed in Table I, which shows that the

copper and sulfur contents in the sample are 17.82 and 8.07 wt pct, respectively. The content of magnetite in the sample is approximately 12.9 wt pct.

Four different phases in the slag sample can be observed by using an electron probe X-ray microanalyzer (EPMA), as shown in Figure 1. The fayalite phase with a long strip shape is the base of the slag; the white grey particles consisting of copper, iron and sulfur elements are the matte phase, which has a large particle size (> 100 μm). Many magnetite particles are distributed in the slag, and the matte particles are attached to the magnetite particles. Energy-dispersive X-ray spectroscopy (EDS) analysis shows that the copper grade of the matte is approximately 57 wt pct. Based on theoretical calculation, the matte content in the slag sample is 31.26 wt pct, and the calculation formula is expressed in Eq. [1]. The relative content of magnetite is up to 19.0 wt pct when matte is removed from the slag.

$$W_{\text{matte}} = \frac{W_{\text{Cu}}}{M_{\text{matte}}} \times 100 \text{ Pct} \quad [1]$$

where W_{matte} and W_{Cu} are the matte and copper content in the slag, respectively; M_{matte} is the copper content in the matte.

2. Waste cooking oil

Waste cooking oil (WCO) exposures to the natural environment can cause hydrolysis, rancidity and other reactions because of a certain amount of water in the WCO. Using WCO as reductant, the water and impurities in the WCO should be removed prior to injection. Because of the density difference, the oil and water are stratified when the WCO is heated to 60 °C; then, the water in the sublayer is removed by mechanical separation. After removing water, solid impurity particles are filtered from the WCO by Whatman no. 4 filter paper (aperture: 20–25 μm). Table II shows that the C and H constituted 90.14 wt pct of the pre-treated WCO mass. To ensure good fluidity, the WCO is pre-heated to 50 °C before injection.

B. Apparatus and Procedure

The slag-cleaning experiments were carried out in a vertical tube furnace equipped with lifting device, which was designed by our group and manufactured by Henan Chengyi Laboratory Equipment Co., Ltd. First, 300 g of ISASMELT copper slag sample was put into a corundum crucible, and then it was placed in the constant temperature zone of the reactor by a lifting device. After the air in the reactor had been discharged by a vacuum pump, nitrogen (100 mL/min) measured by a mass flow meter (D08-1F, Sevenstar, China) was continuously introduced as the protective gas in the whole experimental process. The WCO lance was inserted into the reactor at a certain depth and heated up with the furnace. When the reactor reached the set temperature (heating rate: 10 K/min) for 40 minute, the WCO began to inject into the slag with the carrier gas. After injection, the lance was slowly raised out of the furnace to prevent it from sticking to the crucible or reactor, and

Table I. Chemical Analysis of the ISASMELT Copper Slag

Component	Cu	Fe (Total)	SiO ₂	S	Al ₂ O ₃	CaO	MgO	Zn	Fe ₃ O ₄
Content Wt Pct	17.82	33.06	19.13	8.07	2.96	2.12	1.95	1.83	12.9

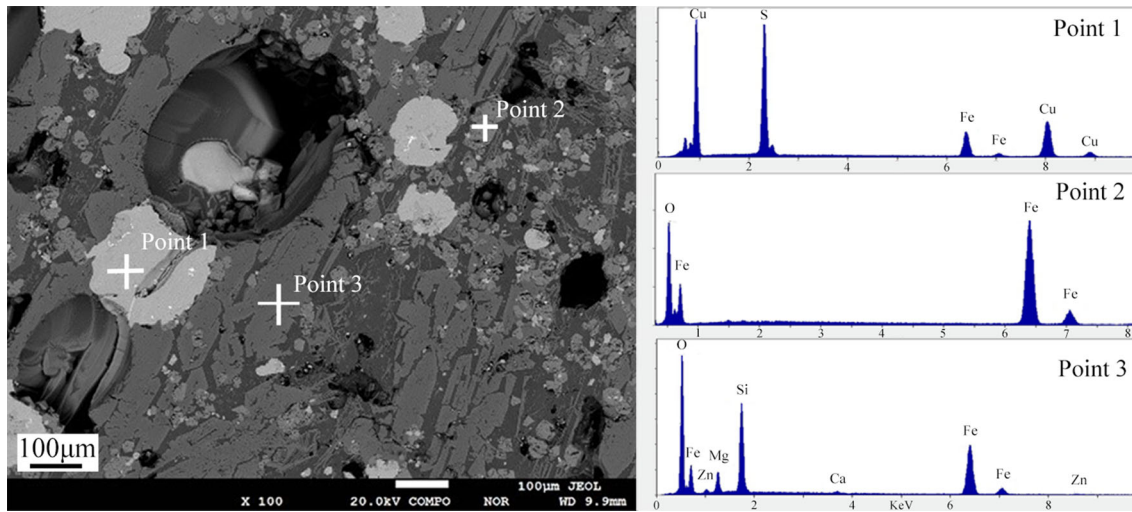


Fig. 1—Microstructure and EDS analyses of ISASMELT copper slag.

Table II. Element Analysis of Waste Cooking Oil

Element	C	H	O	N	S
Content (Wt Pct)	77.81	12.33	8.93	0.86	0.07

the sample was kept in the furnace for cooling. The schematic diagram of the experimental device is shown in Figure 2. The experimental conditions of all tests involved in this study are summarized in Table III.

C. Analytical Method

1. Chemical analysis

The compositions of the copper slag were detected by chemical analysis methods. For different components, different analysis methods were used. The copper content was determined by atomic absorption spectrometry (AAS, SHIMADZU, AA-6300C, Japan). The iron content in the slag was detected with a potassium dichromate titration method; silica content was measured by the gravimetric method; magnesium oxide and calcium oxide were measured by complexometric titration.

2. Elemental analysis of WCO

The quantitative analyses of C, H, N and S within WCO were detected using an elemental analyzer (2400 Series II, PerkinElmer), and the O element content was calculated by the formula:

$$w_O = 100 \text{ Pct} - w_C - w_H - w_N - w_S \quad [2]$$

where w_i is the i (C, H, N, S and O) element content in WCO.

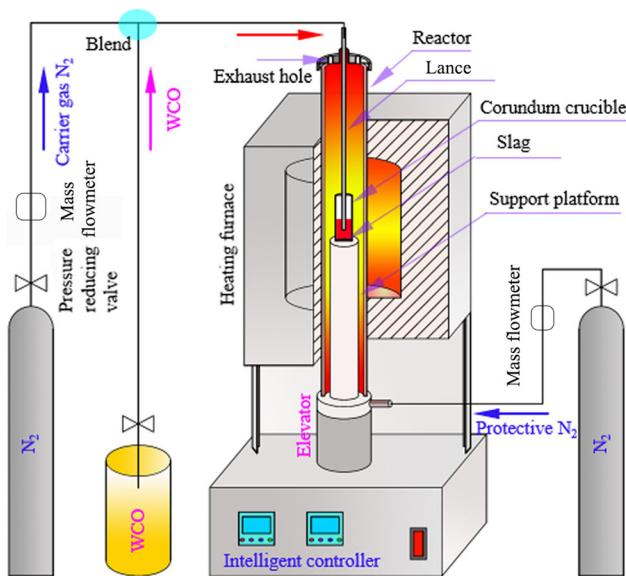


Fig. 2—Schematic diagram of the experimental cleaning device.

3. Instruments

The EPMA (JEOL, JXA 8230, Japan) technique was adopted to analyze the microstructure of the slag sample. The phase in the sample was analyzed using the X-ray diffraction (XRD, Rigaku, D/max-R, Japan) technique, which was conducted on a diffractometer with Cu K α ($\lambda = 1.5406 \text{ \AA}$) radiation; the corresponding diffraction angle was scanned from 10 to 90 deg at a step size of 0.02 deg. A magnetic susceptibility technique (SATMAGAN 135, Rapiscan Systems, Finland) was used to determine the Fe₃O₄ content in the slag sample with an accuracy of ± 0.4 pct.

III. RESULTS AND DISCUSSION

A. Theoretical Basis

The main components of fayalite-based copper slag are iron oxides (FeO and Fe₃O₄) and SiO₂. Based on the slag compositions, the phase equilibrium of this ISASMELT copper slag during the smelting process was analyzed by a FeO-Fe₃O₄-SiO₂ ternary phase diagram (depicted by thermodynamics Factsage software). Figure 3 shows a small liquid phase region (yellow area) exists in the phase diagram at 1250 °C. Combined with the chemical analysis result (Table I), the component point of the ISASMELT copper slag is located in the three-phase coexistence region (liquid, spinel and SiO₂) in equilibrium state, indicating that the solid spinel phase (dominated by Fe₃O₄) precipitates from slag. Fe₃O₄ with a high melting point is beneficial to lining protection; nevertheless, excessive Fe₃O₄ in the slag deteriorates the conditions of matte settling from slag. To ensure reasonable cleaning conditions, the content of Fe₃O₄ in slag is commonly controlled within 5 wt pct,^[2] and the slag component point shifts from the “Liq + Spinel + SiO₂” region (green area in Figure 3) towards the liquid phase region (yellow area in Figure 3). Based on the previous report,^[13] excessive reduction of Fe₃O₄ should be avoided in the reduction process because the formation of metallic iron in the slag will form foaming slag because of the increase in the slag's viscosity.

Reduction is a direct way to decrease the Fe₃O₄ content in slag. H₂, CO, C and CH₄ are the main cracking products of WCO at high temperature.^[12] The reducibility of these reductants is beyond doubt. Reduction of iron oxides and/or other metal oxides with H₂, CO and C as reductants has been extensively investigated.^[14–17] Many scholars have made extensive research on H₂ and CO as reductants, demonstrating that H₂ has better reducibility at high temperature ($> 810 \text{ °C}$).^[18] However, the reduction behaviors interact with each other as both carbon and H₂ exist in the reduction system, and water produced by reduction of H₂ may react with C to generate CO and H₂ again at cleaning temperature ($\text{H}_2\text{O} + \text{C} \rightarrow \text{H}_2 + \text{CO}$, $\Delta_r H_m > 0$). H₂ also can convert CO₂ into water and CO ($\text{H}_2 + \text{CO}_2 \rightarrow \text{H}_2\text{O} + \text{CO}$, $\Delta_r H_m > 0$). Higher temperature encourages the two endothermic reactions to proceed in the positive direction, and H₂ acts as a

transport medium as a result. In addition, with low H₂ density, it is easily volatilized under the action of the high-temperature carrier gas in the reactor. Therefore, the utilization ratio of H₂ in the actual cleaning process will be reduced, and the CO and C may act as the main reductants. The reduction process of copper slag is the reduction of magnetite to ferrous oxide, which is part of an endothermic reaction. An increase in temperature could be beneficial to increasing the reductant efficiency. For methane, secondary cracking of methane occurs at high temperatures, and the corresponding products are hydrogen and carbon.^[19] The reducibility of methane has been confirmed in previous reports.^[15]

B. High-Temperature Separation

Three hundred grams of ISASMELT copper slag was directly sedimented at 1250 °C for 70 minute and then cooled with the furnace. The vertical section of the cooled sample and its microstructure are shown in Figure 4. Two separate layers are observed after separation, corresponding to the slag and matte layers. Furthermore, the slag layer in Figure 4 presents two different structures by macroscopic observation. A large number of pores exist in the upper part of the slag (Figure 4(a)), leading to a loose structure, whose microstructure is similar to that of the original slag (Figure 1). Four phases can be observed in the slag layer, namely, matte, fayalite, magnetite and amorphous glass phases. Matte particles in the upper slag have a high aggregation degree with a large size ($> 200 \mu\text{m}$) and are attached to the magnetite particles. At 1250 °C, magnetite is difficult to melt into liquid phase completely, resulting in an increase in the slag viscosity. With the escaping SO₂ gas (generated from Reaction [3]), foaming slag is formed in the upper layer. The SO₂ gas is discharged from bottom to top, so that Reaction [3] in the lower layer proceeds in the positive direction. The Fe₃O₄ in the lower slag is gradually consumed, and the viscosity decreases as a result. Therefore, the foaming slag phenomenon disappears and the structure becomes compact. The SEM image indicates that fayalite and magnetite are the dominant phases; meanwhile, partial matte particles are accumulated in the slag with a small particle size (Figure 4(b')). The dark red part at the bottom of the sample is matte phase based on the SEM analysis (Figure 4(c')).



Quantitative analyses of the magnetite and copper content in the slag layer were carried out by a magnetic analyzer and chemical analysis method, respectively. The results are given in Figure 4. The magnetite content in the upper part of the slag (Figure 4(a)) reaches approximately 18.6 wt pct, and the high magnetite content confirms the cause of foaming slag formation. The corresponding copper content is 15.43 wt pct, which is close to that in the original slag (17.82 wt pct). For the lower slag layer (Figure 4(b)), the content of magnetite is 10.2 wt pct. Fayalite-based copper slag has a certain

Table III. List of Experimental Conditions of all Tests

Experimental Type	Parameter	Parameter Range	Fixed Parameters			
			T	V_{WCO}	t	P_{lance}
High Temperature Separation	—	—	1523	—	70	—
Determination of Lance Position	above the slag layer	—	1523	4	30	- 1
	below the slag layer	—	1523	4	30	+ 1
Reduction and Settling	T (K)	1503, 1523, 1543, 1563	—	3	60	+ 1
	V_{WCO} (mL)	1.4, 1.8, 2.2, 2.6, 3.0, 3.4	1523	—	60	+ 1
	t (min)	30, 60, 90, 120	1523	2.2	—	+ 1

T Reduction temperature (K), V_{WCO} WCO dosage (mL), t settling time (min); P_{lance} lance position, - 1 1 cm above the slag layer, + 1 1 cm from the bottom of the crucible.

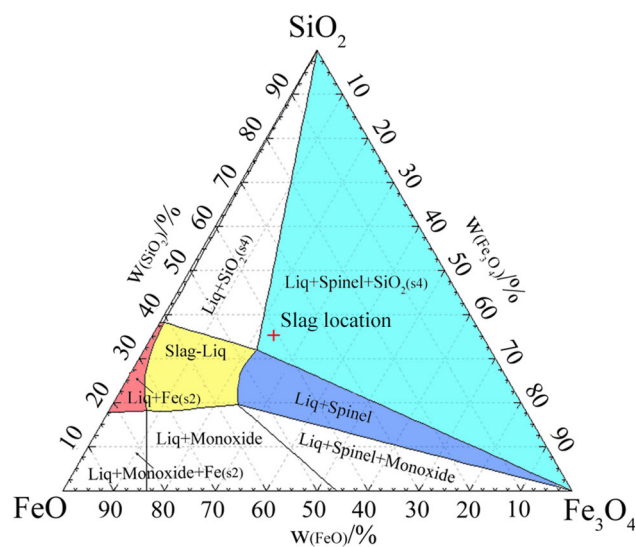


Fig. 3—Ternary diagram of FeO-Fe₃O₄-SiO₂ at 1250 °C.

solubility to magnetite, thereby avoiding the formation of foaming slag and reducing the copper content in the slag significantly ($w_{Cu} = 3.89$ wt pct).

C. Determination of the Lance Position

Combined with the above analyses, the matte cannot efficiently separate from the copper smelting slag by settling without reduction. The upper part of the slag forms foaming slag because of the large amounts of magnetite, and this is in line with the phase equilibrium analysis (Figure 3). Even though no foaming slag is formed in the middle layer, the copper content in the slag still reaches 3.89 wt pct. From the theoretical viewpoint, reducing magnetite helps to remit spinel phase precipitation, and the slag viscosity reduces accordingly. Injection of WCO into the slag layer during the cleaning process might be an effective way to reduce magnetite in the slag. The position of the lance has a certain relationship with the cleaning effect. The practical production indicates that a mushroom head forms at the nozzle by inserting the lance into the molten slag layer, reducing its service life. Placing the lance above

the liquid slag level may result in poor contact between the reductants and the melt. Therefore, the influence of the two positions on the cleaning effect is discussed.

1. Injection above the slag layer

After 300 g of the copper smelting slag was heated at 1250 °C for 40 minute, the lance was placed 1 cm above the surface of the molten slag. The injection rate of WCO was 2 mL/min for 2 minute, and N₂ was used as a carrier gas (3 L/min). After injection, the slag was kept for 30 minute and then cooled with the furnace. Compared with Figure 4, the thickness of the upper foaming slag layer decreases and the compact slag layer increases after reduction (Figure 5). The microstructure of each layer in Figure 5 is similar to the results of Figure 4. Large particles of matte aggregate in the foaming slag layer (Figure 5(a')) with copper content of 15.53 wt pct, and the corresponding magnetite content is 17.2 wt pct. While the matte particle size in the compact slag layer is fine and fayalite has good crystallinity, the magnetite and copper content in this slag layer decreases to 8.7 and 2.76 wt pct, respectively (Figure 5).

Theoretical analysis shows that the reductive products produced by 4 mL WCO cracking are sufficient to reduce the magnetite to FeO. As WCO was injected into the surface of the slag layer, it was difficult for the gas flow to the drive melt stirring. Thus, the H₂, CO and C produced by WCO cracking cannot be completely mixed with the slag, and the utilization ratio of WCO is low as a result. Slag containing large amounts of magnetite cannot achieve the purpose of slag cleaning.^[20]

2. Injection below the slag layer

The lance was inserted into the slag layer with its tip 1 cm from the bottom of the crucible in this set of the experiment, and the vertical section of sample after reduction is shown in Figure 6. The slag sample was divided into the matte layer and slag layer, and the foaming slag disappeared. The magnetite content is approximately 1.7 wt pct in the slag layer, and the corresponding copper content decreases to 1.25 wt pct (Figure 6). This result is in line with the SEM-EDS analysis, which indicates that the few matte and magnetite particles are distributed in the slag (Figure 6(a)).

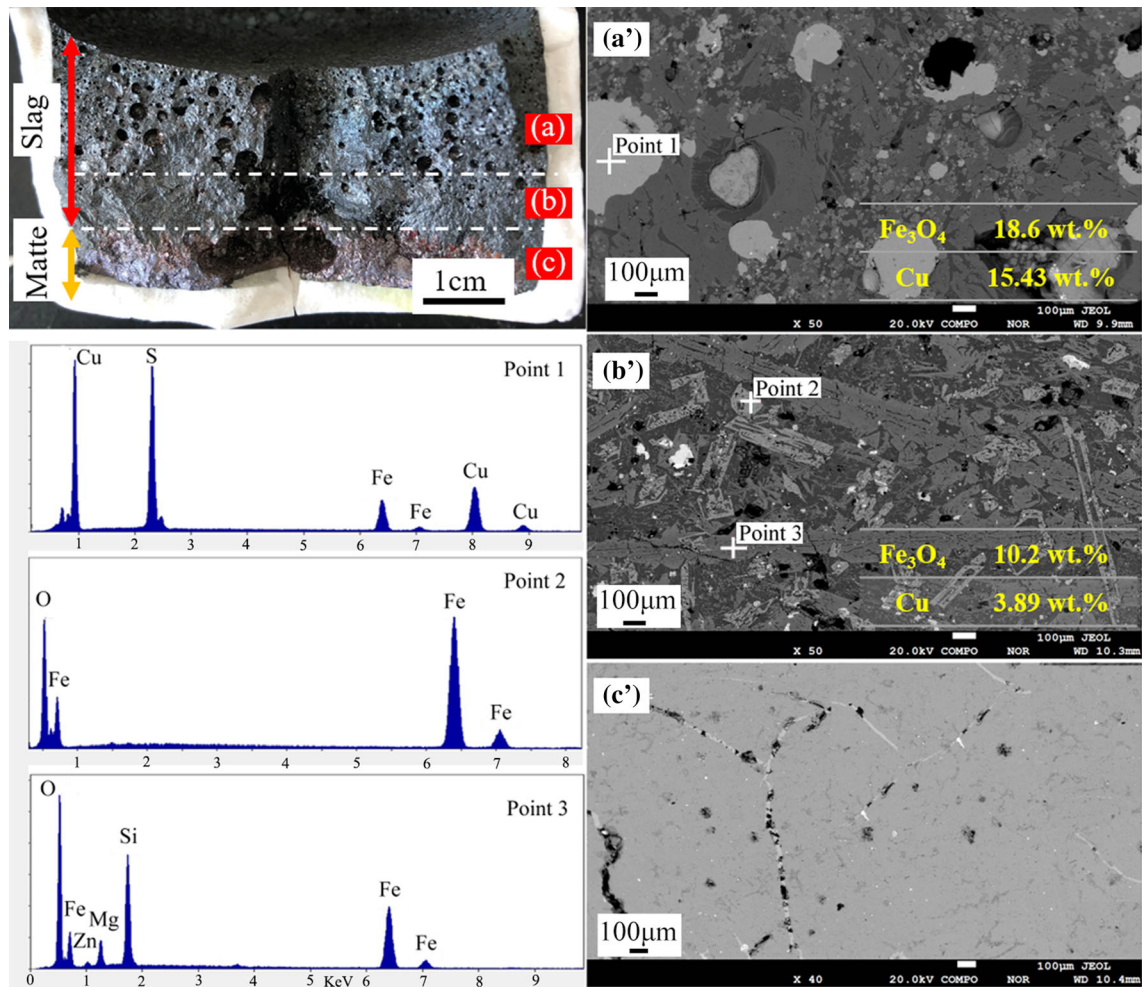


Fig. 4—Vertical section and its SEM-EDS images of the sample after separation at 1250 °C for 70 min; (a'), (b') and (c') correspond to the microstructure of (a), (b) and (c), respectively.

Figure 7 simulates the mixing and stirring of the melt with cracked products of WCO when the WCO was injected into the surface and internal area of the melt. As WCO is injected into the slag surface (Figure 7(a)), the reductants produced by cracking cannot mix with the melt and are distributed on the slag surface, resulting in a decreasing reaction interface between the reductant and magnetite. As WCO is injected into the slag internal, the melt is stirred strongly with the gas flow. The contact of the reductants and magnetite in the slag is strengthened and the reduction effect promoted as a result. This phenomenon demonstrates that WCO injected into the internal slag can make it participate in the reduction well. A decrease in magnetite content will indirectly reduce the slag viscosity and avoid the formation of foaming slag, thereby accelerating the matte particle settling. Therefore, the lance is selected for insertion into the internal slag layer to carry out slag cleaning experiments.

D. Reduction and Settling

1. Effect of the reduction temperature

Figure 8 shows the magnetite content of the slag reduced with 3 mL WCO (injection rate: 1.5 mL/min; injection time: 2 minute) at various reduction temperatures ranging from 1230 °C to 1290 °C and then settling for 60 minute. The result indicates that the magnetite content in slag decreases from 6.9 to 2.0 wt pct as the reduction temperature increases from 1230 °C to 1250 °C. An increase in temperature will intensify the thermal motion between molecules, and the reduction of magnetite to ferrous oxide by H₂ and/or CO belongs to the endothermic reaction.^[18] Thus, the higher temperature is beneficial to reducing the magnetite. Further increasing the temperature to 1290 °C, the magnetite content decreases slightly with a value of 1.1 wt pct. This likely occurs because the distribution of magnetite in the slag is dispersed with decreasing content. The contact

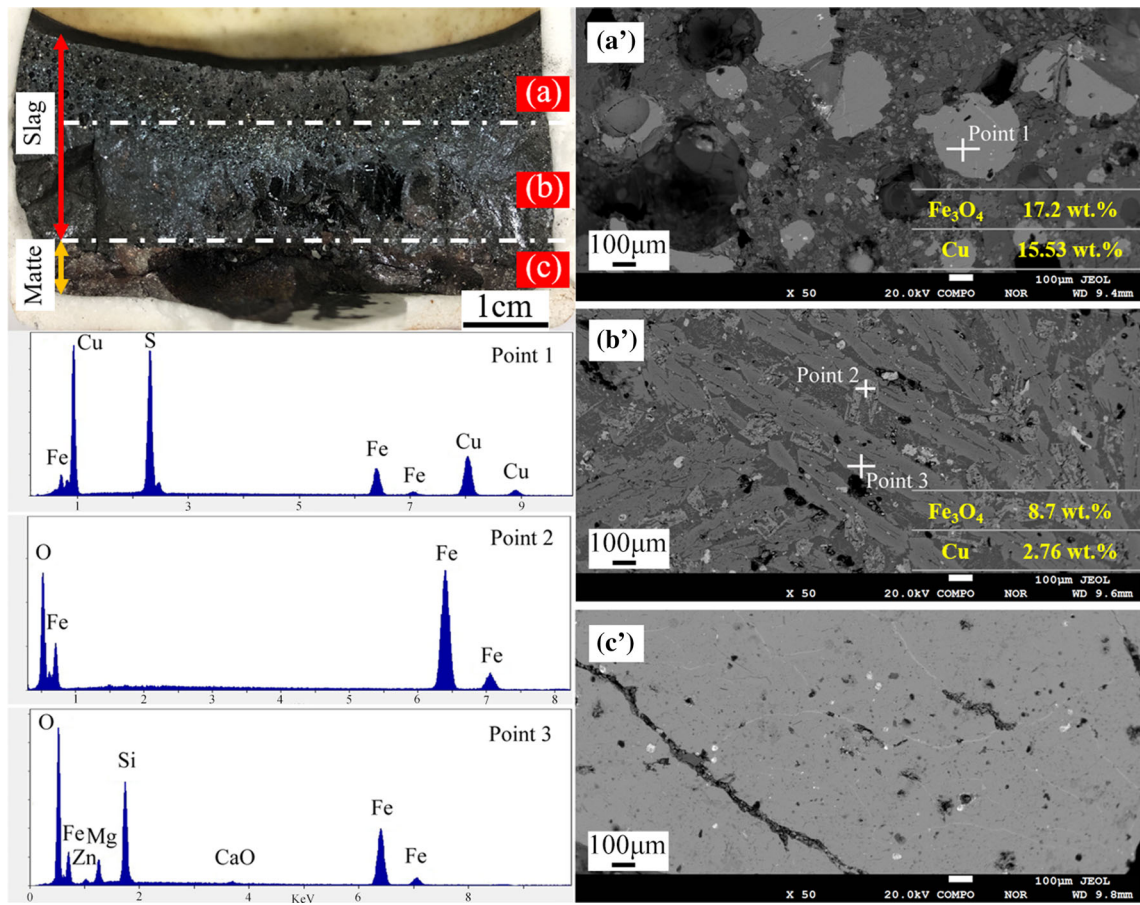


Fig. 5—Vertical section and SEM-EDS images of the sample after reduction with WCO by injection above the slag layer; (a'), (b') and (c') correspond to the microstructure of (a), (b) and (c), respectively.

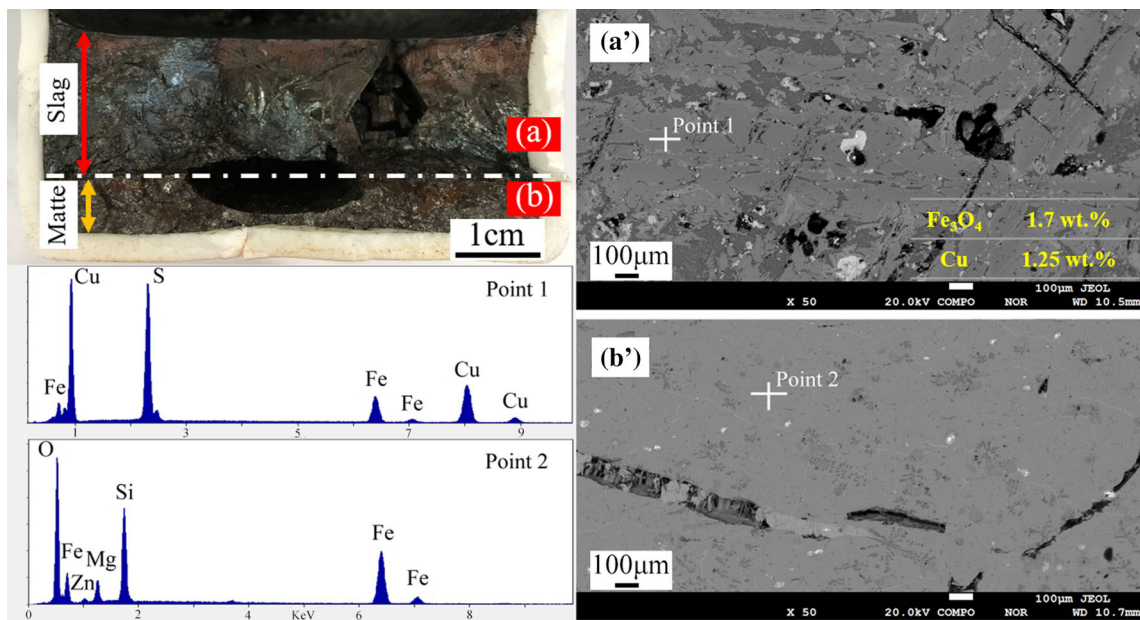


Fig. 6—Vertical section and SEM-EDS images of the sample after reduction with WCO by submerged injection; (a') and (b') correspond to the microstructure of (a) and (b), respectively.

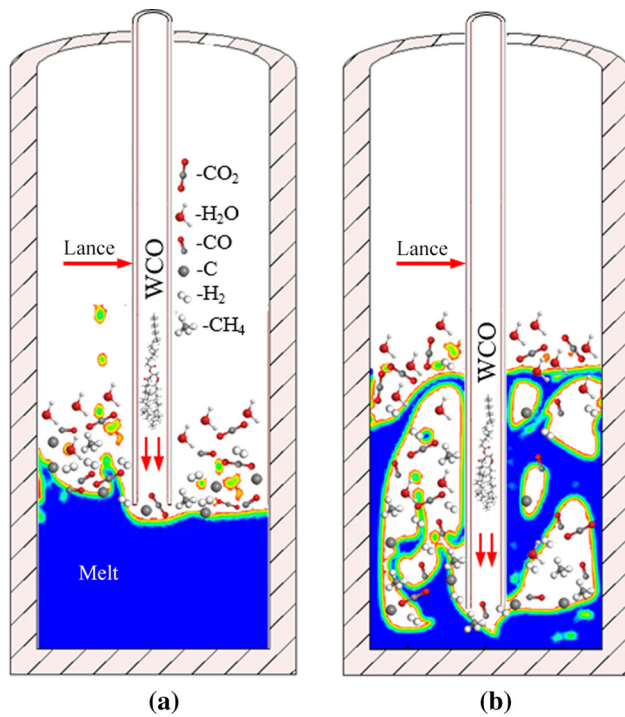


Fig. 7—Simulated image of WCO injection, (a) injection above the surface; (b) submerged injection.

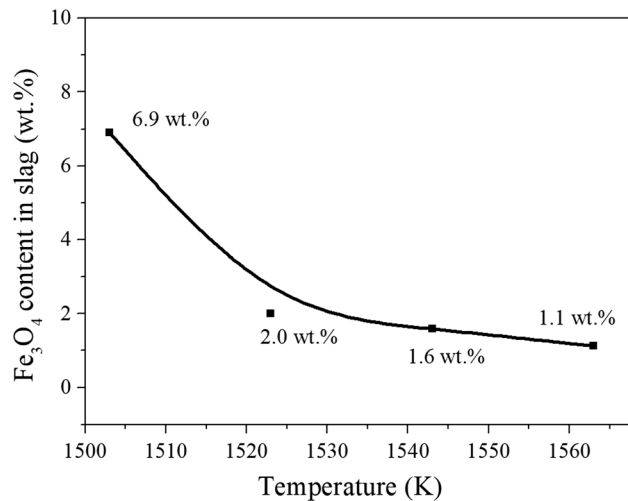


Fig. 8—Fe₃O₄ content in slag as a function of temperature after injection of 3 mL WCO with an injection rate of 1.5 mL/min.

opportunity between the reductants and magnetite is reduced, which makes magnetite difficult to further reduce. Copper slag cleaning in an industrial electric furnace commonly reduces the magnetite to < 5 wt pct,^[2] which ensures that the slag is in a proper viscosity range for promoting matte settling and lining protection simultaneously.

The XRD pattern shows that the magnetite diffraction peaks disappeared in the slag sample after reduction under the above conditions at 1250 °C (Figure 9), indicating good reduction of the slag using WCO. In addition, the copper-bearing phase is also difficult to

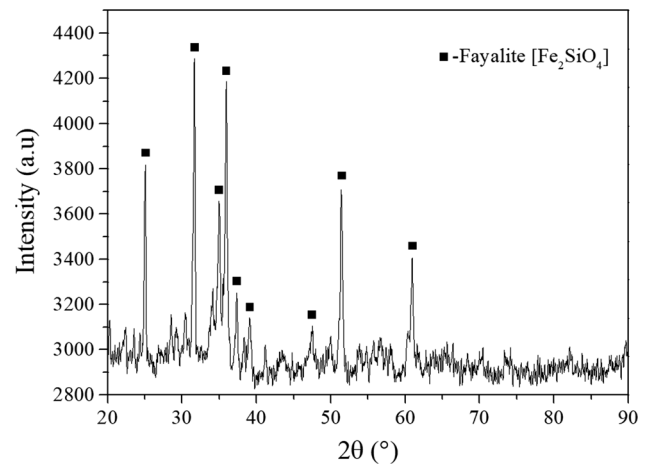


Fig. 9—XRD pattern of the reduced slag sample.

detect, and fayalite becomes the major phase. Based on the results of SEM-EDS analysis (Figure 10), partial matte particles still are distributed in the slag, and occasionally larger matte particles (> 200 μm) are observed. This may be attributed to the insufficient settling time during slag cleaning. The magnetite phase is dispersed and fine in Figure 10, which is consistent with the results of the magnetic analysis and XRD pattern.

2. Effect of WCO dosage

Complete reduction of magnetite to FeO in the slag requires only 1.04 mL WCO upon theoretical calculation; the computing method has been reported previously,^[12] which converted C, H and S in WCO into CO₂, H₂O and SO₂. As a matter of fact, CO gas will be generated during the reduction process, and WCO cannot be fully utilized. The effect of WCO dosage on the magnetite content was investigated to determine the reduction characteristics of WCO under the present conditions.

Thermal cracking converts WCO into small molecular products, offering the reductants for the reduction process. With increasing WCO dosage, the contact opportunities between the reductants (H₂, CO, C, CH₄) and magnetite increased. Figure 11 presents the magnetite content reduced by various dosages of WCO (0 to 3.4 mL) at 1250 °C and then settling for 60 minute. The magnetite content in the slag decreased significantly at first and then stabilized with increasing WCO dosage. Specifically, the magnetite sharply decreases from 19.0 to 7.1 wt pct by adding 1.4 mL of WCO. In theory, the reductive products generated by 1.04 mL of WCO are sufficient to reduce Fe₃O₄ to FeO. However, partial gas products, especially lighter reductants such as H₂ and CH₄, escaped from the reactor with the carrier gas, which reduces the utilization ratio. As the WCO further increases to 2.2 mL, the magnetite decreases slightly to 3.2 wt pct. This may be attributed to the poor kinetic reaction condition after the reduction reaction enters the later stage. Thus, the magnetite in slag decreases slowly and eventually tends to becoming steady at WCO dosage > 2.2 mL.

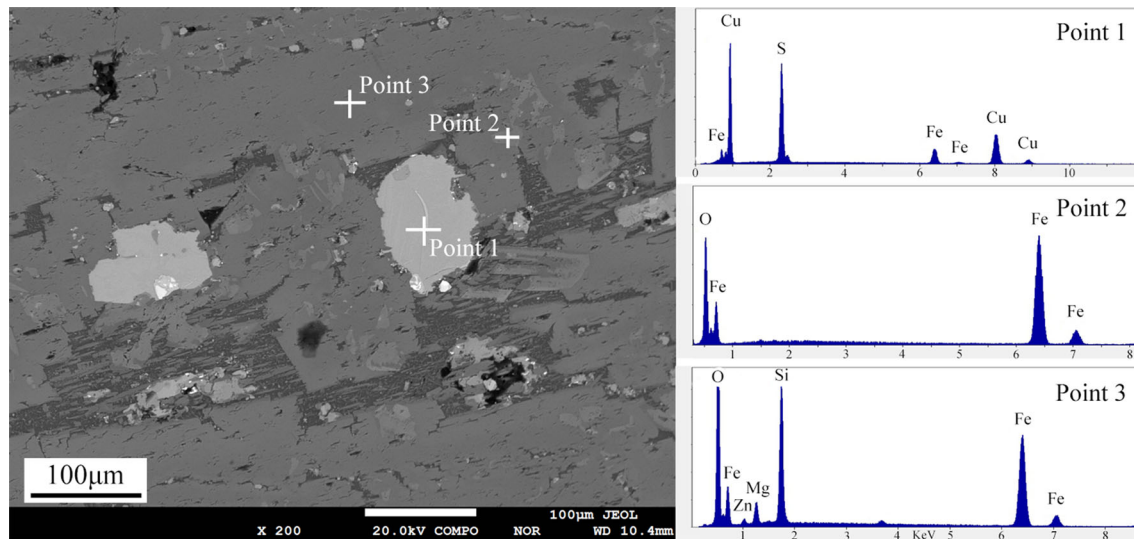


Fig. 10—SEM image of the reduced slag sample.

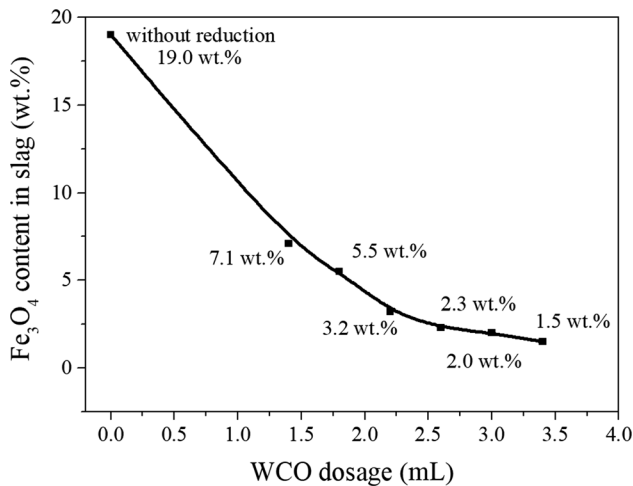


Fig. 11—Fe₃O₄ content in slag as a function of WCO dosage after reduction at 1250 °C.

3. Effect of settling time

The magnetite content in the slag can be reduced to approximately 3 wt pct by reasonably controlling the temperature and the WCO dosage. Nevertheless, settling at high temperature after reduction is one of the critical steps for copper slag cleaning in an electric furnace. After settling, the longitudinal section of the slag layer in the sample was evenly cut into three layers to determine the magnetite and copper content in each layer. The results of the magnetite content of each slag layer reduced by 2.2 mL WCO at 1250 °C as a function of settling time (30 to 120 minute) are shown in Figure 12(a), and the corresponding copper contents are depicted in Figure 12(b). Prolonged settling time has no obvious effect on the magnetite content, which fluctuates between 2–4 wt pct. This phenomenon demonstrates that the reduction reaction mainly occurs in the injection WCO stage, and the distribution of magnetite in the slag layer is uniform.

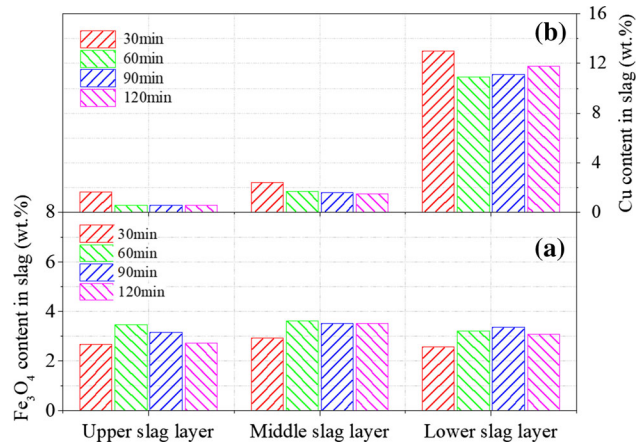


Fig. 12—Contents of Fe₃O₄ and Cu in each slag layer as a function of settling time, (a) Fe₃O₄ content; (b) Cu content.

The matte particles descend from top to bottom in the slag, resulting in the gradient distribution of the copper in the slag layer. Small particle size presents a slow settling rate based on the Stokes equation.^[21] Within 30 minute of settling time, partial small matte particles could not settle completely, and the corresponding copper contents in upper, middle and lower slag were 1.65, 2.42 and 12.98 wt pct, respectively. Prolonging the time provides favorable conditions for the settling. The copper content in the upper slag descends to 0.55 wt pct to prolong the settling time to 60 minute; nevertheless, further increasing in settling duration, the copper content remains at approximately 0.55 wt pct. This part of the copper is mainly due to the chemical dissolution of copper.^[22] The copper loss in the slag can be divided into mechanical entrainment loss and chemical dissolution loss.^[1] Prolonging the time can effectively reduce the mechanical entrainment loss of copper in the slag. However, chemically dissolved copper is related to the physicochemical properties of the copper slag. Based on

the theoretical calculation (Eqs. 4-9),^[23-25] the chemical dissolution loss of copper in the present slag is approximately 0.51 wt pct (oxidation state: 0.38 wt pct; sulfidation state: 0.13 wt pct) as the magnetite in the slag is reduced to approximately 3 wt pct. Therefore, the copper content in the slag cannot be reduced to < 0.5 wt pct by reduction without changing the properties of the slag. As a matter of fact, the slag can be discarded when the copper content is decreased to < 0.57 wt pct in actual industrial copper production.

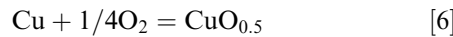
$$(\text{Pct Cu})_t = (\text{Pct Cu})_O + (\text{Pct Cu})_S \quad [4]$$

where $(\text{Pct Cu})_t$ is the total dissolved Cu in the slag; $(\text{Pct Cu})_O$ is the oxidation state dissolved Cu in the slag; $(\text{Pct Cu})_S$ is the sulfidation state dissolved Cu in the slag.

The oxidation state dissolved Cu in the copper slag can be calculated by the formula^[23]:

$$(\text{Pct Cu})_O = 29.73 a_{\text{CuO}_{0.5}} \quad [5]$$

Based on the reaction,



$$K = \frac{a_{\text{CuO}_{0.5}}}{P_{\text{O}_2}^{1/4} a_{\text{Cu}}} \quad [7]$$

Thus, $a_{\text{CuO}_{0.5}}$ can be expressed as follows:

$$a_{\text{CuO}_{0.5}} = K \times a_{\text{Cu}} \times P_{\text{O}_2}^{1/4} \quad [8]$$

where $a_{\text{Cu}} \approx 1$, P_{O_2} can be calculated by Factsage.

The sulfidation state dissolved Cu in the slag can be calculated by the formula^[24,25]:

$$(\text{Pct Cu})_S = 0.00495 [\text{S}]_{\text{Sl}} [\text{Cu}]_{\text{mt}} \quad [9]$$

where $[\text{S}]_{\text{Sl}} = 2.2 - 3.75X + 1.26X^2$, $X = 0.01[\text{Cu}]_{\text{mt}}$, and $[\text{Cu}]_{\text{mt}}$ is the matte grade.

For the lower slag layer, the copper content is > 10 wt pct; in particular, the settling time is prolonged to 120 minute, and the value is still as high as 11.78 wt pct. The lower slag layer contacts the matte layer directly, providing conditions for the reaction between the matte and slag components. The generated gas (SO_2) may entrain part of the matte into the lower slag during the discharge process. In addition, the bottom surface of the slag adsorbs some matte particles, which also increases the copper content of the lower slag (the specific reason will be analyzed in detail in the next section). Therefore, the copper content in the lower slag is higher.

E. Copper Distribution After Cleaning

1. SEM-EDS analysis of the cleaned slag

To investigate the distribution of copper in the slag after cleaning, Figure 13 shows the microstructures of each slag layer after reduction and settling for 120 minute. As seen from the SEM images coupled with the EDS results, fayalite, presented in charcoal gray, is the

main phase in the reduced slag. The distributions of copper phase in each layer are in accordance with the chemical analysis. A small amount of copper-bearing phase (consists of Fe, Zn, Cu, S elements) distributes in the upper layer of slag; the fine particles disperse uniformly in the amorphous glass phase (Figure 13(a')). This part of the copper should be attributed to the chemically dissolved copper described previously, which precipitates during the cooling process. In the middle layer, the spinel phase (iron-aluminum spinel, namely, FeAl_2O_4) encapsulated with the matte particle can be observed occasionally (Figure 13(b')). This finding explains the reason why the copper content in this layer is relatively high (> 1 wt pct). Matte particle size in the lower layer has a significant increase, as shown in Figure 13(c'). Existing in the form of mechanical entrainment with large particle size (> 200 μm) confirms the results of the chemical analysis in Figure 12.

2. Slag-matte interface

Analysis results mentioned above indicate that the copper content in the lower slag layer is high. In addition to the mechanical entrainment copper in the internal slag layer, many macroscopic matte particles are adsorbed on the bottom surface of the slag layer (Figure 14). Furthermore, Figure 15 presents the EPMA images of the slag-matte interface after reduction and settling (reduction temperature 1250 °C, 2.2 mL WCO dosage, settling duration 120 minute). Spinel phase present in Fe_3O_4 and FeAl_2O_4 has been observed between the slag layer and matte layer based on the WDS analysis. Ferrous oxide (FeO) is reflected in the actual WDS analysis results (Figure 15); this can be attributed to Reaction (3), which indicates Fe_3O_4 would be reduced to low-valent iron oxide once it comes in contact with the matte.

For FeAl_2O_4 , the formation may be due to the compositions of the slag. Table I shows that the Al_2O_3 content within the slag is 4.36 wt pct. After reduction, the relative content of Al_2O_3 in the slag will increase because of the removal of oxygen and matte from the slag. The compositions of the reduced slag sample (middle slag layer in the aforementioned experimental conditions) are list in the Table IV, in which the Al_2O_3 relative content enhances to 6.39 wt pct. From the viewpoint of thermodynamics, the Gibbs free energy of the FeAl_2O_4 formation ($\text{FeO} + \text{Al}_2\text{O}_3 \rightarrow \text{FeAl}_2\text{O}_4$) decreases with the drop of temperature, while the corresponding equilibrium constant increases (Figure 16). Therefore, the slow cooling process provides favorable thermodynamic conditions for the precipitation of FeAl_2O_4 spinel. Furthermore, the oxygen potential of the system decreases after reduction, which is more conducive to the formation of FeAl_2O_4 .^[26]

Spinel and matte phases have good wettability,^[27] and encapsulation may occur when they come in contact with each other, as shown in Figure 13(b). In addition, the contact between the two phases prevents the matte from falling off from the slag layer, leading to the

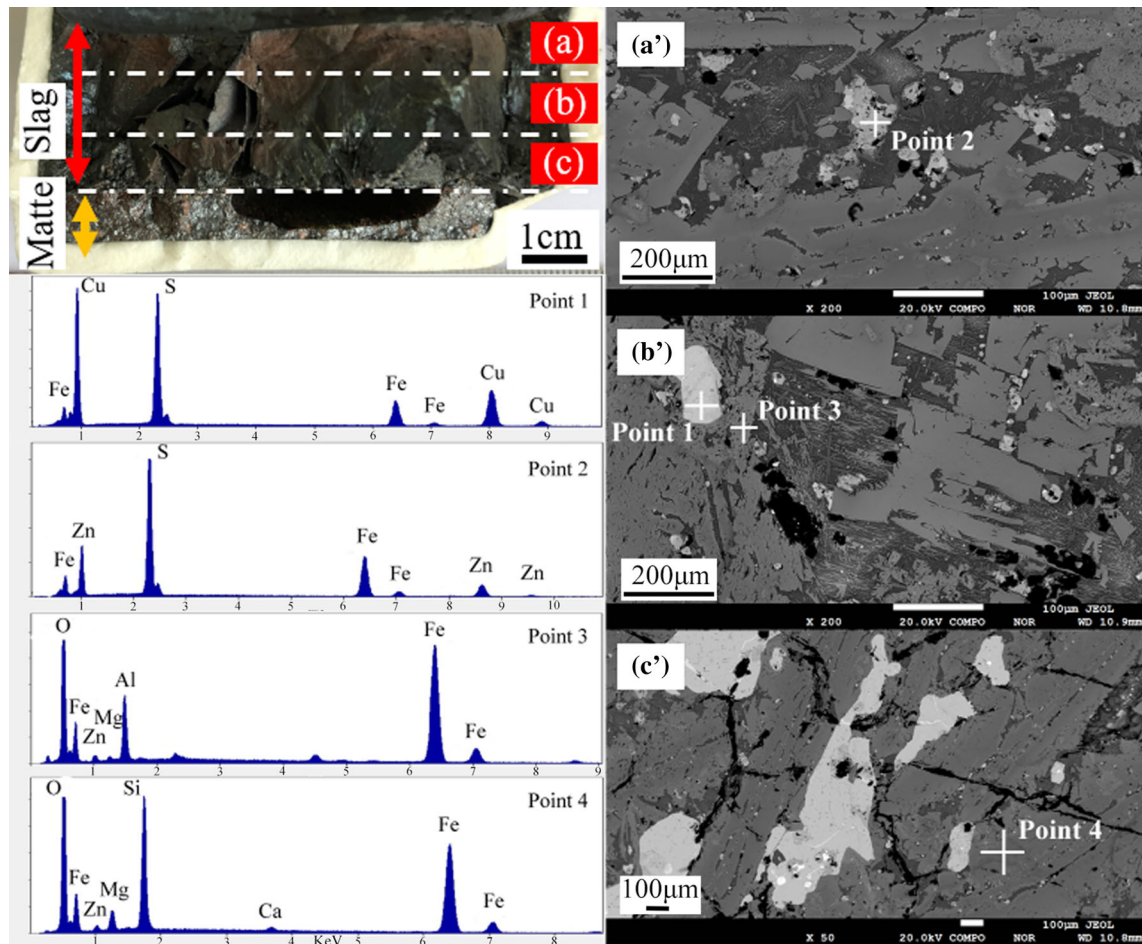


Fig. 13—Vertical section and its SEM-EDS images of the sample after reduction and settling at 1250 °C for 120 min; (a'), (b') and (c') correspond to the microstructure of (a), (b) and (c), respectively.

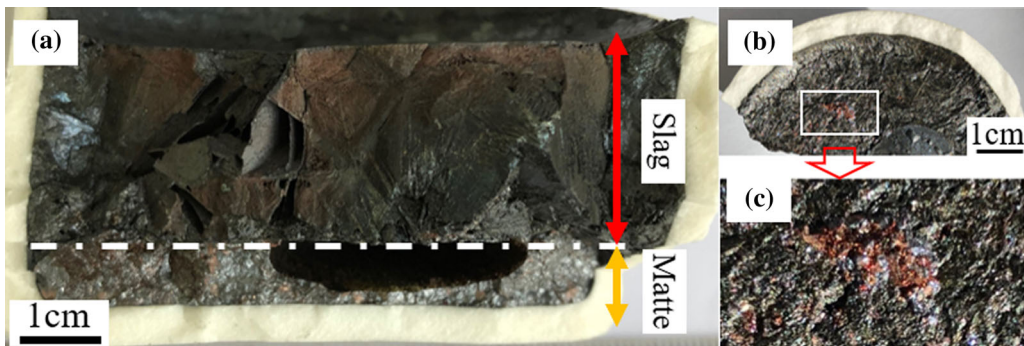


Fig. 14—Vertical section image of the slag sample after reduction and separation for 120 min (a); (b): bottom surface of the slag layer; (c): white area enlargement in (b).

increase in copper content in the lower slag. Thus, the spinel phase between the slag layer and matte layer is the key factor hindering the mechanical separation of the matte layer from the slag layer.

IV. CONCLUSIONS

Excessive magnetite in the slag causes foaming slag, hindering the separation of matte from the slag. H₂, CO and C produced by WCO cracking can be used as a direct reductant to reduce the magnetite in the slag.

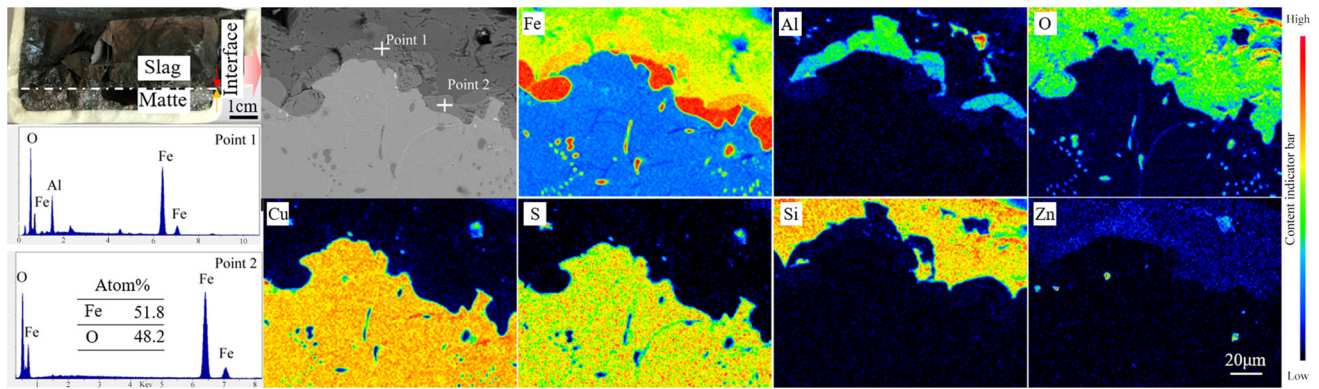


Fig. 15—Vertical section image of the slag and EPMA analysis of the interface between the slag layer and matte layer.

Table IV. Chemical Analysis of the Middle Slag Layer After Reduction and Settling for 120 Min

Component	Cu	Fe (Total)	SiO ₂	S	Al ₂ O ₃	CaO	MgO	ZnO	Fe ₃ O ₄
Content (Pct)	1.50	41.48	27.18	1.53	6.39	4.17	3.45	3.01	3.5

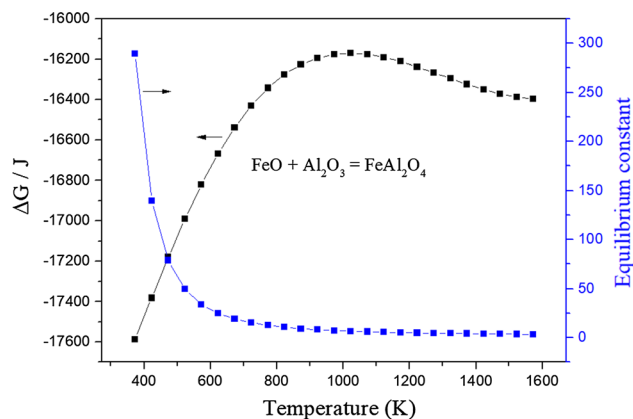


Fig. 16—Changes in the Gibbs free energy and equilibrium constant of the formation reaction of spinel.

After cleaning, the copper content distributed in the slag increases from top to bottom in the direction of the longitudinal section. Copper in the upper layer of the ISASMELT copper slag (300 g) can be decreased from 17.82 to 0.56 wt pct *via* reduction at 1250 °C for settling 60 minute in the presence of 2.2 mL WCO, followed by cooling with the furnace, and the corresponding magnetite content was approximately 3 wt pct. The copper contents in the middle and lower slag layer are 1.68 and 10.89 wt pct, respectively. The slow cooling process provides favorable thermodynamic conditions for the precipitation of FeAl_2O_4 spinel from the melt. The wetting phenomenon between the spinel and matte hinders the settling of the matte. The results obtained in present study indicate that WCO can be used as a reductant to realize green cleaning and solve the issues of non-renewable reductant resources and carbon neutralization in the cleaning process.

ACKNOWLEDGMENTS

This work was supported by the National Natural Science Foundation of China (51664039 and U1602272); China Scholarship Council (the International Clean Energy Talent Program, 2017).

REFERENCES

- R. Sridhar, J.M. Toguri, and S. Simeonov: *Metall. Mater. Trans. B.*, 1997, vol. 28B, pp. 191–200.
- S. Demetrio, S.A.J. Ahumada, M.Á. Durán, E. Mast, U. Rojas, J. Sanhueza, P. Reyes, and E. Morales: *JOM*, 2000, vol. 52, pp. 20–25.
- A. Warczok, G. Riveros, P. Echeverriá, C.M. Díaz, H. Schwarze, and G. Sánchez: *Can. Metall. Q.*, 2013, vol. 41, pp. 465–73.
- N. Karimi, R. Vaghar, and M.R.T. Mohammadi: *J. Inst. Eng. India Ser. D.*, 2013, vol. 94, pp. 43–50.
- A. Sarrafi, B. Rahmati, H.R. Hassani, and H.H.A. Shirazi: *Miner. Eng.*, 2004, vol. 17, pp. 457–59.
- U. Kumar, S. Maroufi, R. Rajarao, M. Mayyas, I. Mansuri, R.K. Joshi, and V. Sahajwalla: *J. Clean. Prod.*, 2017, vol. 158, pp. 218–24.
- S. Zhou, Y. Wei, B. Li, and H. Wang: *J. Clean. Prod.*, 2019, vol. 217, pp. 423–31.
- Z. Zuo, Q. Yu, M. Wei, H. Xie, W. Duan, K. Wang, and Q. Qin: *J. Therm. Anal. Calorim.*, 2016, vol. 126, pp. 481–91.
- S. Chen and L. Xu: *China Food Drug Adm. Mag.*, 2018, vol. 4, pp. 50–53 (In Chinese).
- C.D. Mandolesi de Araújo, C.C. de Andrade, E. de Souza e Silva and F.A. Dupas: *Renew. Sustain. Energy Rev.*, 2013, vol. 27, pp. 445–52.
- M.J.A. Romero, A. Pizzi, G. Toscano, G. Busca, B. Bosio, and E. Arato: *Waste Manag.*, 2016, vol. 47, pp. 62–68.
- S. Zhou, Y. Wei, S. Zhang, B. Li, H. Wang, Y. Yang, and M. Barati: *J. Clean. Prod.*, 2019, vol. 236, p. 117668.
- S. Zhou, Y. Wei, B. Li, and H. Wang: *Metall. Mater. Trans. B.*, 2018, vol. 49B, pp. 3086–96.
- J. Oh and D. Noh: *Fuel*, 2017, vol. 196, pp. 144–53.
- H. Zhang, X. Shi, Z. Bo, and H. Xin: *Metall. Mater. Trans. B.*, 2014, vol. 45B, pp. 582–89.
- J.H. Heo, B.S. Kim, and J.H. Park: *Metall. Mater. Trans. B.*, 2013, vol. 44B, pp. 1352–63.

17. W.K. Jozwiak, E. Kaczmarek, T.P. Maniecki, W. Ignaczak, and W. Maniukiewicz: *Appl. Catal. A*, 2007, vol. 326, pp. 17–27.
18. X. Huang: *Principles of Iron and Steel Metallurgy*, 3rd ed., Metallurgical Industry Press, Beijing, 2002, pp. 418–19 (In Chinese).
19. H.J. Grabke: *Metall. Trans.*, 1970, vol. 1, pp. 2972–75.
20. R. Sridhar, J.M. Toguri, and S. Simeonov: *JOM*, 1997, vol. 49, pp. 48–52.
21. P.K. Iwamasa and R.J. Fruehan: *ISIJ Int.*, 1996, vol. 36, pp. 1319–27.
22. P. Coursol, N. Cardona Valencia, P. Mackey, S. Bell, and B. Davis: *JOM*, 2013, vol. 64, pp. 1305–13.
23. J.M. Toguri and N.H. Santander: *Can. Metall. Q.*, 1969, vol. 8, pp. 167–71.
24. P.J. Mackey: *Can. Metall. Q.*, 1982, vol. 21, pp. 221–60.
25. M. Nagamori: *Metall. Trans.*, 1974, vol. 5, pp. 531–38.
26. C. Liu: *Physical Chemistry of Copper Metallurgy*, Science and technology of China press, Beijing, 1990, pp. 600–02 (In Chinese).
27. N. Eustathopoulos, M.G. Nicholas, and B. Drevet: *Wettability at High Temperatures*, Pergamon, Oxford, 1999.

Publisher's Note Springer Nature remains neutral with regard to jurisdictional claims in published maps and institutional affiliations.